Analyzing Quantum Noise in Image Encodings: A Circuit-Based Hybrid Integration Approach

Yayu Mo

Mitchell A. Thornton

Sanjaya Lohani

Southern Methodist University (SMU) Dallas, Texas, USA yayum@smu.edu

Electrical and Computer Engineering Darwin Deason Institute for Cyber Security Electrical and Computer Engineering Southern Methodist University (SMU) Dallas, Texas, USA mitch@smu.edu

Southern Methodist University (SMU) Dallas, Texas, USA slohani@smu.edu

Abstract—Quantum information technologies are reshaping communication systems, but reliable integration of classical data, particularly images, into quantum frameworks remains a challenge. Circuit-based quantum image encoding methods are susceptible to noise-induced degradation, which undermines reproducibility and reliability. Here, we investigate the impact of quantum noise channels across the encoding and measurement stages within a hybrid quantum-classical distributed system. We also introduce noise into selected gate operations and measurements to demonstrate its distinct effects on the quantum circuit. To quantify the results, we compute the mean squared error (MSE), the structural similarity index measure (SSIM), and the peak signal-to-noise ratio (PSNR), and benchmark the results across various settings of the noise parameter. Finally, we present experimental results highlighting how image complexity affects encoding robustness using the Linnaeus and MNIST datasets. We anticipate that the presented results will contribute to the development of dependable quantum-classical orchestration strategies for resilient image processing.

Index Terms-quantum noise channel, quantum data embedding, quantum image representation, quantum distributed system

I. INTRODUCTION

Encoding classical images into quantum states has emerged as a significant research direction in quantum computing and quantum communication, aiming to leverage the advantages of quantum parallelism and entanglement. However, inherent noise in quantum systems, such as decoherence, operational errors, and environmental interactions, poses substantial challenges to preserve the fidelity of quantum encoded and decoded images.

Numerous studies have investigated the effects of noise on various quantum algorithms. At the beginning of the 1970s, Hellwig and Kraus [1, 2] formalized general quantum noise channels and modeled noise as quantum operations arising from environmental interactions. In 1997, Barenco et al. [3] examined the relationship between environmental noise and quantum error correction algorithms, highlighting that simulating noise in encoded states can aid in the design of appropriate correction mechanisms. They also introduced models that involve dephasing and arbitrary noise as part of their framework. Also in 2010, Quek et al. [4] analyzed how phase noise, defined as the combined effects of phase noise and other noise channels, contributes to the phenomenon of

entanglement sudden death in Bell states. Additionally, in our previous work [5], we showed a connection of classical noise to quantum image processing based on the general angle encoding scheme.

However, traditional quantum encoding schemes, such as basis encoding and angle encoding, often demand more qubits than current quantum simulators can support. For example, the Qiskit QASM simulator is limited to 30 qubits, yet encoding a 32×32 image using basis encoding would require 32×32×8 qubits to represent every pixel. Furthermore, encodings such as amplitude encoding exhibit a massive circuit depth as data scales, severely undermining execution efficiency due to the decomposition of high-dimensional matrices. To address this bottleneck and facilitate a classical-quantum hybrid framework, we develop a distributed architecture, illustrated in Fig. 1. Our method consists of a multistage hybrid classicalquantum processing: First, we resize the images and send them to a classical management system, which partitions the data stream and distributes them across available quantum nodes (Qnodes). Second, each Qnode encodes its image partition and transmits the encoded quantum state through noisy quantum channels. After that, we obtain expectation values by taking enough measurements to achieve statistical confidence. In the final step, the measurements data are collected in a classical memory and subsequently reassembled to reconstruct the encoded image.

Building on the concept outlined in the preceding paragraph, our contribution advances channel noise analysis in two distinct dimensions. First, we shift the focus from conventional quantum state fidelity [6, 7] to examining the direct impact of noise models on quantum image encoding schemes. Second, our integration of a hybrid distributed quantum-classical architecture offers a promising foundation for developing nextgeneration noise-resilient quantum strategies.

The remainder of this paper is organized as follows. Section II presents our proposed approach and experimental setup, including a description of the dataset used. Section III presents the experimental results, supported by both visual and quantitative analysis. Finally, Section IV concludes the paper and outlines directions for future research.

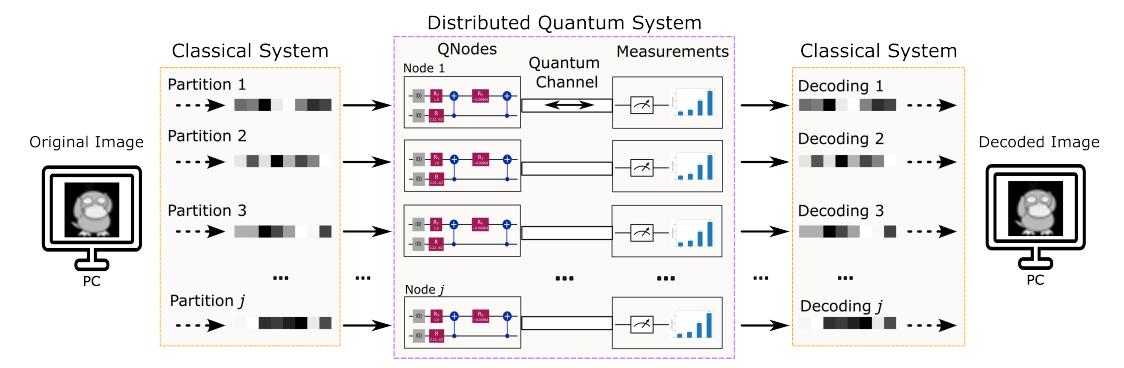


Fig. 1: Multistage hybrid classical—quantum distributed image processing framework. Noise is introduced during pixel encoding at Qnodes and during quantum channel transmission prior to measurement.

II. APPROACH

A. Image encoding under channel noise

We use the amplitude encoding method as a major encoding scheme throughout the paper. This scheme encodes data into amplitude coefficients based on their coordinates. In the context of image representation, the encoding is defined by the following density matrix form:

$$\rho_f = \sum_{i,j} c_i c_j^* |i\rangle \langle j|, c_{i,j} = \frac{F_{i,j}}{\sum (F_{i,j})^2},$$
 (1)

where $F_{i,j}$ denotes the pixel value at the position of (i,j). Based on the encoding scheme, the embedded channel noise could be expressed as

$$\varepsilon(\rho) = tr_E(\sum U_E \rho U_E^{\dagger}). \tag{2}$$

Here, U_E represents the unitary operators that characterize the transformation of the density matrix under noise. The specific forms of U_E corresponding to the noise channels that we explore in the paper are given as,

$$\begin{aligned} & \text{Bit-Flip: } U_E = \sqrt{p}X, \sqrt{1-p}I; \\ & \text{Depolarizing: } U_E = \sqrt{\frac{p}{4}}X, \sqrt{\frac{p}{4}}Y, \sqrt{\frac{p}{4}}Z, \sqrt{1-\frac{3p}{4}}I; \\ & \text{Phase Damping: } U_E = \begin{bmatrix} 1 & 0 & 0\\ 0 & \sqrt{1-\lambda} \end{bmatrix}, \begin{bmatrix} 0 & 0\\ 0 & \sqrt{\lambda} \end{bmatrix}, \\ & \text{Amplitude Damping: } U_E = \sqrt{p_1} \begin{bmatrix} 1 & 0 & 0\\ 0 & \sqrt{1-\gamma} \end{bmatrix}, \sqrt{p_1} \begin{bmatrix} 0 & \sqrt{\gamma}\\ 0 & 0 \end{bmatrix} \\ & \sqrt{1-p_1} \begin{bmatrix} \sqrt{1-\gamma} & 0\\ 0 & 1 \end{bmatrix}, \sqrt{1-p_1} \begin{bmatrix} 0 & 0\\ \sqrt{\gamma} & 0 \end{bmatrix}, \end{aligned}$$

where p, p_1, λ, γ denote the noise parameters associated with their respective channels.

As illustrated in Fig. 1, the scheme introduces noise at both the Qnode and measurement junctions. Noise arising at the Qnode is associated with gate operations (gate stage) used during the encoding of data into quantum states. Subsequently, as the encoded image propagates through the quantum channel toward the measurement stage, it is further subjected to

channel-induced noise. In the final stage, we perform measurements using the Pauli-Z basis and calculate the expectation values for each qubit based on their coordinates. These values are then normalized to reconstruct the corresponding pixel intensities.

B. Evaluating Noise Effects

In order to statistically analyze how the distributed circuit mitigates channel noise in embedded images, we use the structural similarity index measure (SSIM). The SSIM is defined as

$$SSIM(x,y) = \frac{(2\mu_x \mu_y + c_1)(2\sigma_{xy} + c_2)}{(\mu_x^2 + \mu_y^2 + c_1)(\sigma_x^2 + \sigma_y^2 + c_2)},$$
 (4)

where μ denotes the mean value of pixels. The terms σ_x^2 and σ_y^2 , respectively, represent the sample variances calculated from individual windows of x and y. The sample covariance between these windows is denoted by σ_{xy} . To ensure numerical stability when the denominator is small, the constants c_1 and c_2 are introduced. These constants are functions of the dynamic range L of the pixel values. Specifically, c_1 and c_2 are defined as

$$c_1 = (k_1 L)^2, \quad c_2 = (k_2 L)^2,$$
 (5)

where $k_1=0.01$ and $k_2=0.03$ are two default constant coefficients.

To assess the impact of noise across a broad dynamic range, we compute the peak signal-to-noise ratio (PSNR), which quantifies the ratio between signal power and noise power as follows:

$$PSNR(x,y) = 10 \log_{10} \frac{\max(x_{i,j})^2}{MSE}$$
 (6)

where $\max(x_{i,j})$ represents the maximum pixel value of the quantized image.

III. RESULTS

A. Noise behavior on various noise channels

For the test image (Psyduck) shown in Fig. 3 (a), we apply amplitude damping to the gate and measurement stages. We

find uniform image-space noise at the thermal excitation population $p_1 = 0.5$ in amplitude damping experiments, so this setting is used throughout the paper. We begin by employing a single-partition encoding scheme in which the entire flattened image is embedded into the quantum state space. Additionally, we compare performance across other quantum noise channels, including phase damping, depolarization, and bit-flip. To analyze the influence of varying parameters, we increase the noise value from 0.05 to 0.35 in increments of 0.05. In addition, to decode high-resolution images, we assign 20,000 shots to the simulator to calculate the expectation values. Due to inherent randomness introduced by quantum noise channels, each experiment is repeated 50 times to calculate the mean SSIM and standard deviation σ , as shown in Fig. 2 (a). Based on the results, we observe the following behaviors: (1) Higher noise parameters degrade image quality; (2) Qnodes and gate operations are more sensitive to noise than the measurement stage; (3) Depolarization exhibits similar characteristics to amplitude damping; (4) The encoding scheme shows relative resilience to both amplitude damping and depolarization.

In a similar manner, we now vary the number of image partitions, each corresponding to an individual quantum processor, Qnode, to facilitate parallel execution, while maintaining a fixed amplitude damping parameter of 0.2. As the number of distributed Qnodes increases, the noise artifacts in the encoded images progressively diminish, as evidenced by the rising SSIM values shown in Fig. 2 (b).

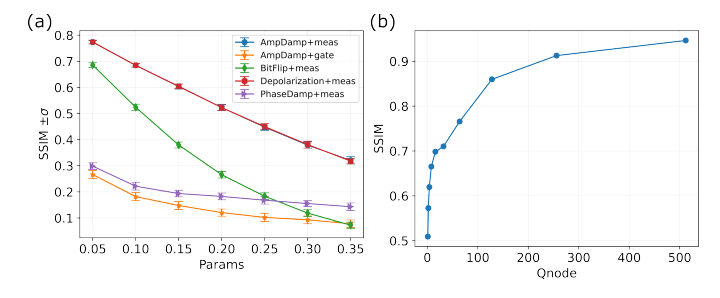


Fig. 2: Evaluation Results. (a) SSIM at various noise parameters. The error bar shows one standard deviation from the mean. (b) Distributed system: SSIM at various Qnodes when noise amplitude parameter is fixed at 0.2.

We present sample output images affected by various quantum noise channels in Fig. 3. From these results, we find several noteworthy patterns: (1) The noise introduced during data encoding into quantum states exhibits a spatial distribution that resembles an approximating behavior from classical Poisson noise; (2) As shown in Fig. 3 (b), (c), and (e), from a direct observation in images, certain patterns resemble Gaussian noise, with a key distinction—Gaussian components tend to be uniformly distributed across the image space, whereas quantum channel noise emanates from localized image regions; (3) Noise applied during gate operations and phase damping manifests itself as highly destructive, effectively erasing key image features within the quantum encoded space.

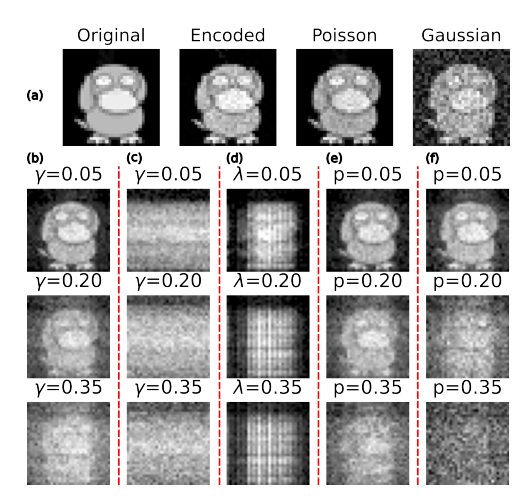


Fig. 3: Output Example Images. (a) Left to right: original image, quantum-encoded image, original image with Poisson noise, original image with Gaussian noise. (b) Amplitude damping in the measurement stage. (c) Amplitude damping in the gates stage. (d) Phase damping. (e) Depolarization. (f) Bit flip.

B. Datasets

To investigate general noise behavior across diverse image types, we evaluate the system using two distinct datasets. In addition to the test image (Psyduck), we employ the Linnaeus-5 dataset [8], which comprises 1600 images of size $256\times256\times3$ per category and is originally curated for classification tasks. Its conformity to the $2^n\times2^n$ dimensional structure aligns well with common quantum encoding requirements. To further examine differences in noise impact between multiple-intensity images and simple-intensity images, we examine a parallel experiment using the MNIST dataset [9] under the same conditions. MNIST includes 60,000 training images and 10,000 testing images of handwritten digits, with a simplified grayscale format of $32\times32\times1$. Notably, its frequency area distribution mirrors that of our primary test image that we used on the circuit and noise model.

C. Experimental Results on Dataset

TABLE I: Dataset experiment result

Subset	AvgMSE	AvgSSIM	AvgPSNR
Linnaeus-berry	1194.950	0.491	17.316
Linnaeus-bird	1225.396	0.435	17.366
Linnaeus-dog	1453.287	0.463	16.958
Linnaeus-flower	1338.535	0.475	16.961
Linnaeus-other	1311.213	0.465	17.147
MNIST-train	2655.868	0.394	14.547
MNIST-test	2870.531	0.395	14.242

To ensure a controlled experimental setting, we preprocess the Linnaeus dataset by converting all images to a single channel and resizing them to 32×32. For the MNIST dataset, rather than utilizing the full set of 60,000 training and 10,000 testing images, we randomly select 1600 images from each subset to match the size of the Linnaeus experiment. To strengthen the reliability of our findings, we incorporate two additional evaluation metrics, MSE and PSNR, to quantify the impact of noise across varying image types. We conduct an experiment using amplitude encoding under an amplitude damping noise model with a parameter value of $\gamma=0.2.$ The results, presented in Table I and illustrated in Fig. 4, reveal distinct patterns in noise behavior and encoding resilience across datasets, offering promising insights for robust quantum image processing.

The results clearly demonstrate that the amplitude damping noise model exerts a stronger influence on images with simple structures and centralized intensity distributions than on more complex images. This behavior can be attributed to the relatively low qubit utilization in the MNIST dataset, where the pixel values are predominantly uniform and background regions contain zero intensity. Consequently, as described in Eq. 3, the amplitude coefficients are more susceptible to interference across unintended qubit positions.



Fig. 4: Examples of encoded images (top-row) and noisy images (bottom-row) in datasets. The first 2 rows are from the MNIST dataset, and the bottom 2 rows are from the Linnaeus dataset.

IV. DISCUSSION

In this paper, we examine the influence of multiple quantum noise channels on image encoding schemes within a quantum distributed system. Departing from conventional approaches that primarily assess fidelity between quantum states, we adopt a direct and intuitive methodology to evaluate the impact of noise through the lens of quantum image encoding. By varying encoding parameters and systematically analyzing output deviations using classical metrics, we uncover consistent patterns that illuminate the behavior of different noise models.

To provide a comprehensive perspective, our experiments incorporate both Qnode-level gate operations and the quantum channels that precede the measurement, capturing the full trajectory of noise propagation. We observe distinct relationships among noise models, particularly in how they disrupt spatial

structures within encoded images. Notably, our comparison with classical noise patterns reveals intriguing parallels: for instance, noise generated during amplitude encoding may exhibit features reminiscent of Poisson or Gaussian distributions, though with markedly different spatial characteristics. Furthermore, as noted in the Qiskit Aer documentation, the amplitude damping channel includes a parameter known as the excited state thermal population, governing the equilibrium population of $|0\rangle$ which can significantly alter the noise behavior. This parameter opens an avenue for further exploration in future work.

We also expand our analysis across diverse datasets to extract generalizable insights. Our results suggest that simpler image structures, especially those with concentrated intensity distributions, are disproportionately affected by amplitude damping noise, underscoring the intricate dependency between circuit encoding depth and image complexity.

We anticipate that our illustrations may pave an exciting step toward robust quantum image processing and quantum-classical co-design. Looking ahead, we aim to validate these findings on real quantum hardware and explore new encoding frameworks that mitigate noise effects during quantum embedding and transmission. These directions hold great promise for the advancement of practical quantum communication and data integration in hybrid systems.

REFERENCES

- [1] K-E Hellwig and Karl Kraus. Pure operations and measurements. *Communications in Mathematical Physics*, 11(3):214–220, 1969.
- [2] K-E Hellwig and Karl Kraus. Pure operations and measurements. *Communications in Mathematical Physics*, 11(3):214–220, 1969.
- [3] Adriano Barenco, Todd A Brun, Rüdiger Schack, and Timothy P Spiller. Effects of noise on quantum error correction algorithms. *Physical Review A*, 56(2):1177, 1997.
- [4] Sylvanus Quek, Ziang Li, and Ye Yeo. Effects of quantum noises and noisy quantum operations on entanglement and special dense coding. *Physical Review A—Atomic, Molecular, and Optical Physics*, 81(2):024302, 2010.
- [5] Yayu Mo, Sanjaya Lohani, and Mitchell Thornton. Distorted edge feature extraction using quantum convolutional structure. In 2025 IEEE 18th Dallas Circuits and Systems Conference (DCAS), pages 1–6, 2025.
- [6] Sangchul Oh, Soonchil Lee, and Hai-woong Lee. Fidelity of quantum teleportation through noisy channels. *Physical Review A*, 66(2):022316, 2002.
- [7] Hao Xiang, Zhang Rong, and Zhu Shi-Qun. Average fidelity of teleportation in quantum noisechannel. *Communications in Theoretical Physics*, 45(5):802, 2006.
- [8] G Chaladze and L Kalatozishvili. Linnaeus 5 dataset for machine learning. *chaladze. com*, 2017.
- [9] Li Deng. The mnist database of handwritten digit images for machine learning research. *IEEE Signal Processing Magazine*, 29(6):141–142, 2012.